# FPGA-based real-time data processing for accelerating reconstruction at LHCb

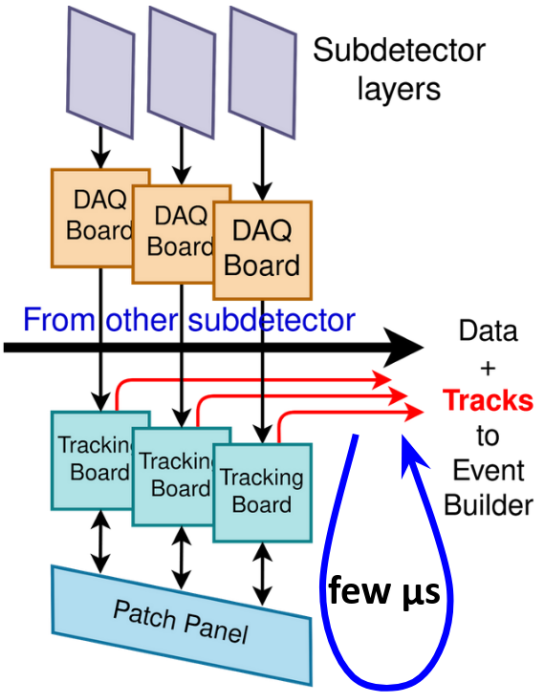


Figure 1: Schematic of the "Artificial Retina" architecture.

| Track type | $\varepsilon$ CPU pat-reco (%) | $\varepsilon$ FPGA pat-reco (%) | |
|---|---|---|---|
| | | all z | fiducial z-region |
| Long tracks with $p > 5$ GeV/c and hits in VELO$> 5$ | $99.84 \pm 0.02$ | $99.27 \pm 0.06$ | $99.45 \pm 0.05$ |
| Long tracks from $b$ with $p > 5$ GeV/c and hits in VELO$> 5$ | $99.61 \pm 0.13$ | $99.24 \pm 0.21$ | $99.41 \pm 0.18$ |
| Long tracks from $c$ with $p > 5$ GeV/c and hits in VELO$> 5$ | $99.89 \pm 0.12$ | $98.50 \pm 0.53$ | $98.62 \pm 0.53$ |

Table 1: Summary of efficiencies of the VELO tracking algorithm for different type of tracks using both the CPU-based and the FPGA-based pattern recognition algorithm. Numbers obtained on 1000 $B_s^0 \to \Phi\Phi$ events. The efficiency is calculated using Long tracks with $2 < \eta < 5$, $p > 5$ GeV/c and with more than 5 hits (Monte Carlo truth) in the VELO detector. Tracks belong to the fiducial region if the z coordinate of the origin vertex is located between -200 mm and 200 mm.

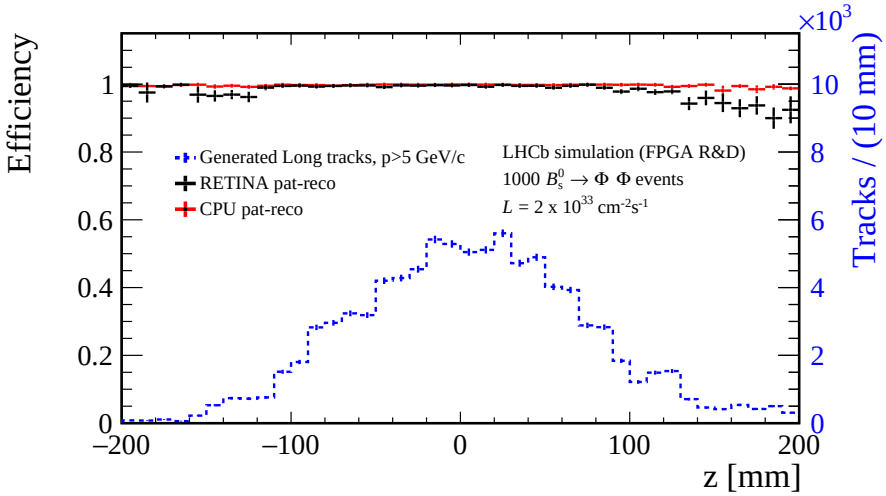


Figure 2: Comparison between VELO tracking efficiencies obtained with the CPU algorithm (VeloClusterTracking) and the RETINA patter recognition algorithm. The efficiency is shown as a function of the z coordinate of the track origin vertex and is calculated on Long tracks (with $p > 5$ GeV and $2 < \eta < 5$). 1000 $B_s^0 \to \Phi\Phi$ events, simulated in LHCb Upgrade conditions, are used to produce the plot. The (scaled) distribution for generated tracks is superimposed on the plot.

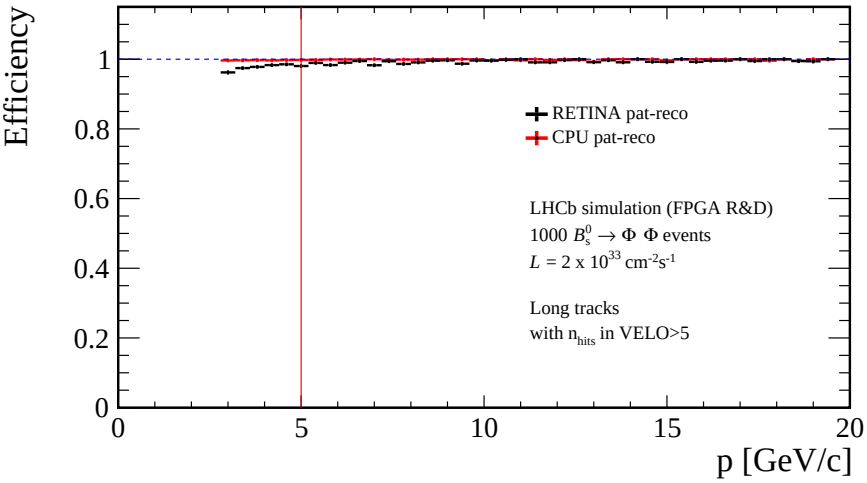


Figure 3: Comparison between VELO tracking efficiencies obtained with the CPU algorithm (VeloClusterTracking) and the RETINA patter recognition algorithm. The efficiency is shown as a function of the momentum of the generated tracks and is calculated on Long tracks ($2 < \eta < 5$) with at least six VELO hits. 1000 $B_s^0 \to \Phi\Phi$ events, simulated in LHCb Upgrade conditions, are used to produce the plot. The red line indicates the cut applied to obtain numbers in Table **??**.

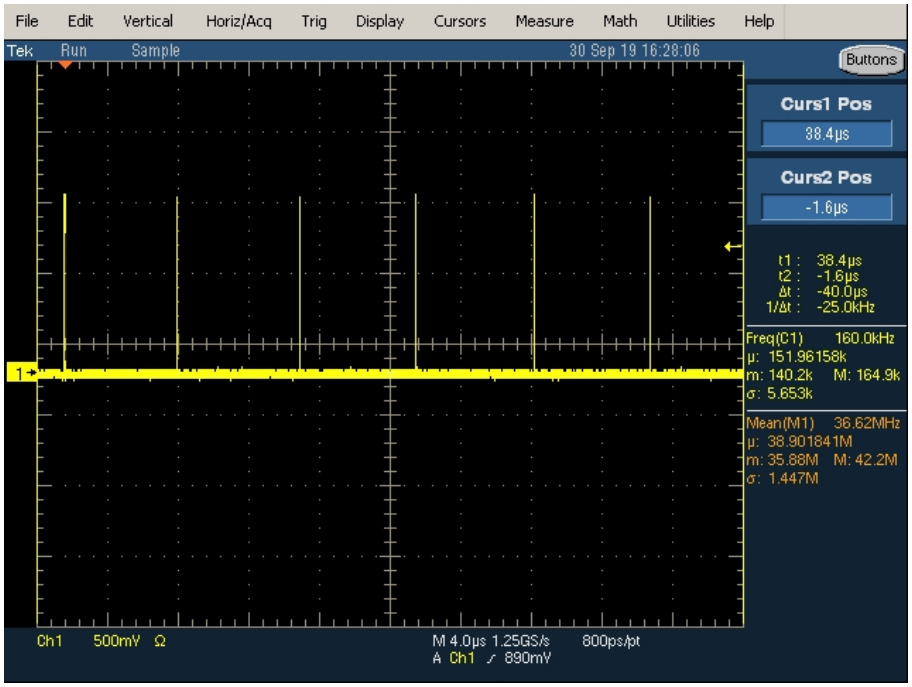


Figure 4: Oscilloscope screen, each spike corresponds to 256 processed events. The measured event rate is 38.9 MHz.

| Track type | Quantity | CPU cluster | FPGA cluster |
|---|---|---|---|
| VELO tracks | efficiency | 98.254% ± 0.007% | 98.257% ± 0.007% |
| | clone | 1.231% ± 0.006% | 1.233% ± 0.006% |
| Long tracks | efficiency | 99.252% ± 0.006% | 99.255% ± 0.006% |
| | clone | 0.806% ± 0.006% | 0.807% ± 0.006% |
| | ghost | 0.848% ± 0.003% | 0.929% ± 0.003% |

Table 2: VELO tracking efficiency, clone and ghost track rates, comparing CPU and FPGA clustering algorithms. Data are 50k minimum-bias simulated events.

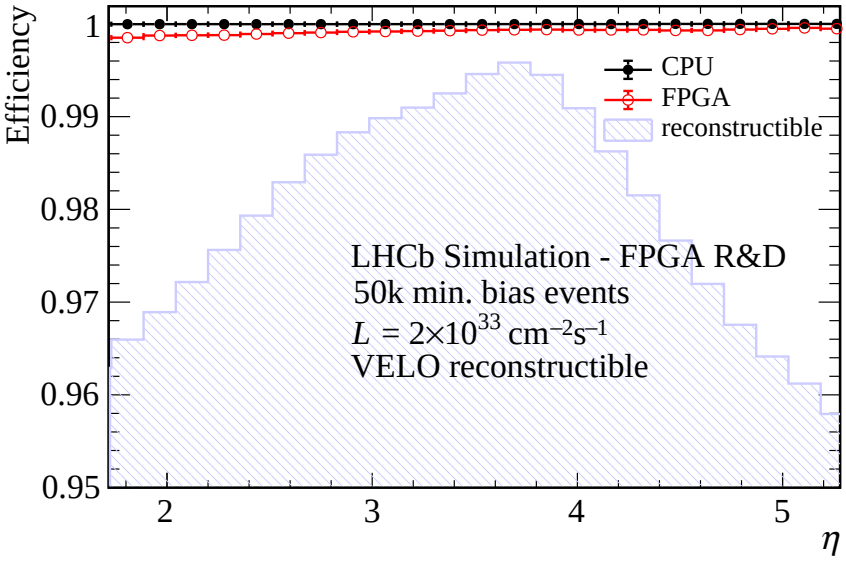


Figure 5: Cluster reconstruction efficiency as function of the pseudo-rapidity, comparing CPU and FPGA algorithms, within the LHCb acceptance ($2 < \eta < 5$). Only clusters from VELO reconstructible tracks are considered. The blue histogram shows the distribution of the detector hits with at least one pixel associated (reconstructible) in pseudo-rapidity. The vertical scale is magnified to highlight the differences between algorithms. Data are 50k minimum-bias simulated events.

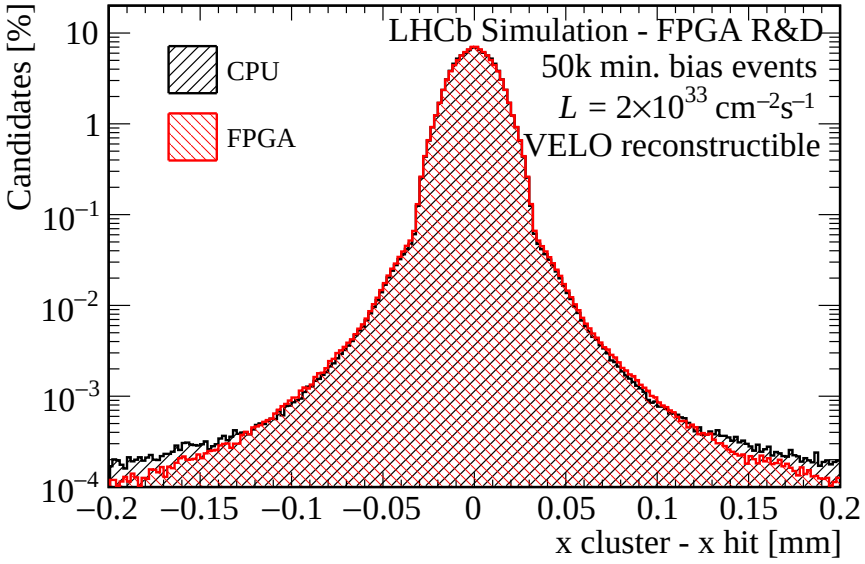


Figure 6: Cluster residual distributions along the $x$ direction, comparing CPU and FPGA clustering algorithms. Only clusters from VELO reconstructible tracks are considered. Data are 50k minimum-bias simulated events.

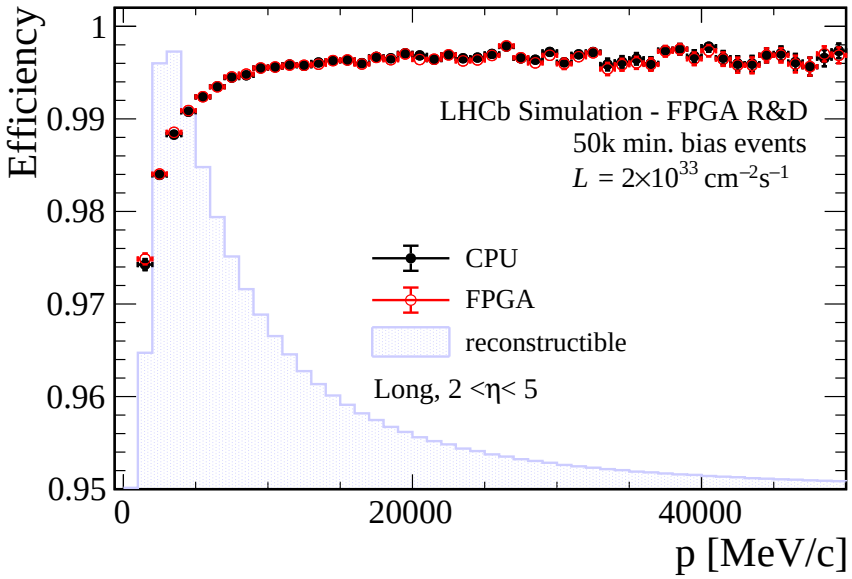


Figure 7: VELO tracking efficiency for long non-electron tracks, matched to a true simulated particle, as a function of the particle momentum, comparing CPU and FPGA clustering algorithms. The blue histogram shows the distribution of the particles in momentum. The vertical scale is magnified to highlight the differences between algorithms. Data are 50k minimum-bias simulated events.

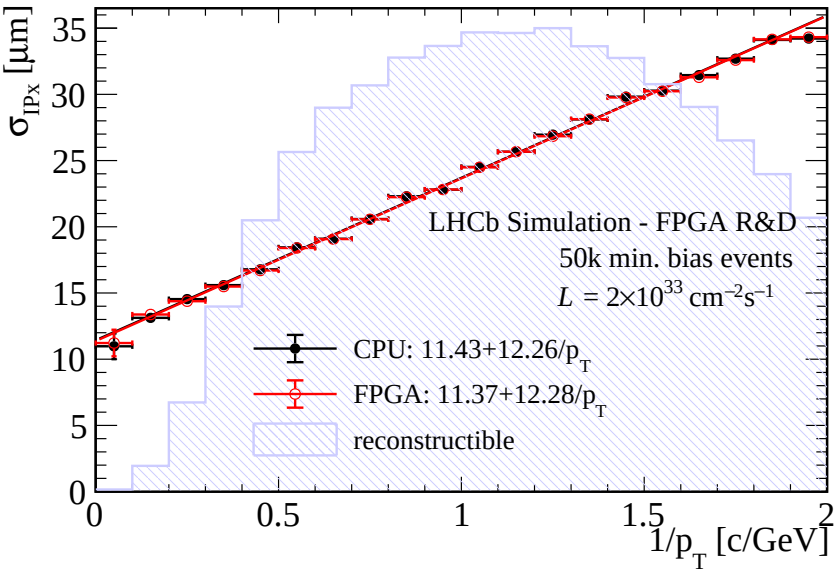


Figure 8: Impact parameter resolution along the $x$ direction for tracks which originated directly in a $pp$ collision, matched to a true simulated particle, as a function of the inverse of the particle transverse momentum, comparing CPU and FPGA clustering algorithms. The results of a linear fit to the CPU and FPGA data sets are also displayed. The blue histogram shows the distribution of the particles in inverse of the transverse momentum. Data are 50k minimum-bias simulated events.

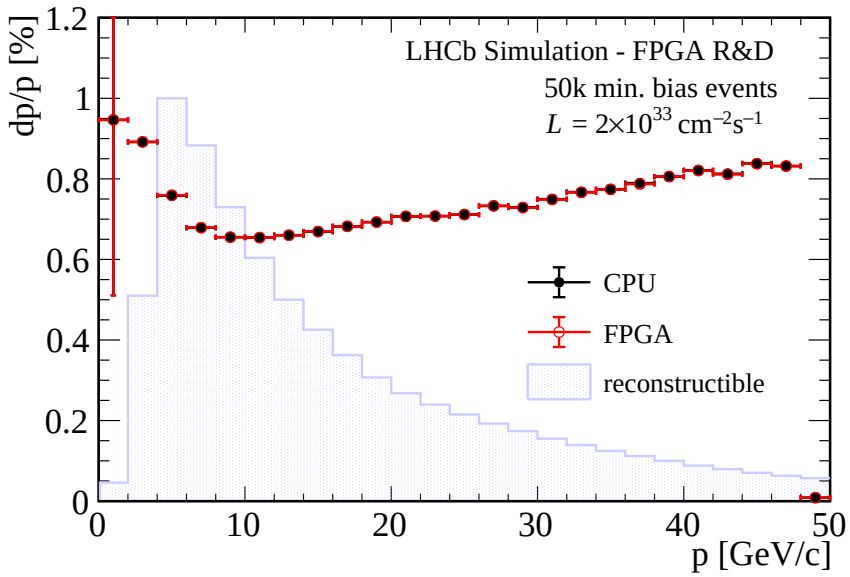


Figure 9: Momentum resolution of forward tracks, matched to a true simulated particle, as a function of the particle momentum, comparing CPU and FPGA clustering algorithms. The blue histogram shows the distribution of the particles in momentum. Data are 50k minimum-bias simulated events.